



ELSEVIER

Contents lists available at ScienceDirect

Journal of Luminescence

journal homepage: [www.elsevier.com/locate/jlumin](http://www.elsevier.com/locate/jlumin)

# Correlation between luminescent characteristics and phase composition of ZnS:Cu powder prepared by self-propagating high temperature synthesis

Yu. Bacherikov<sup>a</sup>, A. Kuchuk<sup>a,\*</sup>, A. Zhuk<sup>a</sup>, Yu. Polischuk<sup>a</sup>, V. Kladko<sup>a</sup>, T. Kryshtab<sup>b</sup>, N. Korsunskaya<sup>a</sup>

<sup>a</sup> V. Lashkaryov Institute of Semiconductors Physics, NAS of Ukraine, 03028 Kyiv, Ukraine

<sup>b</sup> Department of Physics, ESFM-IPN, 07738 Mexico D.F., Mexico

## ARTICLE INFO

### Article history:

Received 6 July 2013

Received in revised form

12 September 2013

Accepted 16 September 2013

Available online 19 September 2013

### Keywords:

Photoluminescence

Phosphors

ZnS

X-ray diffraction

## ABSTRACT

The powder-like ZnS:Cu grown by self-propagating high temperature synthesis from the mixture of Zn, S and CuCl is investigated before and after annealing at 800 °C by photoluminescence (PL) and X-ray diffraction (XRD) techniques. It is found that after synthesis the ZnS:Cu powder consists of a mixture of cubic and hexagonal ZnS phases as well as crystalline  $\text{Cu}_x\text{Zn}_{1-x}$  solid solution. PL spectrum shows a wide PL band which is the superposition of green and blue Cu-related bands as well as self-activated one. It is shown that annealing at 800 °C gives rise to three processes, controlled by the heating time to annealing temperature: (i) phase transformation of ZnS hexagonal phase to cubic one; (ii) oxidation processes resulting in ZnO formation; (iii) the non-monotonic changes of  $\text{Cu}_x\text{Zn}_{1-x}$  phase composition and decrease of its content. These changes are accompanied by the non-monotonic variation of the blue to green Cu-related PL band intensities ratio which correlates with the variation of  $\text{Cu}_x\text{Zn}_{1-x}$  phase composition. The model that explains the changes of ZnS:Cu PL characteristics by indiffusion of Zn and Cu from  $\text{Cu}_x\text{Zn}_{1-x}$  phase is proposed. The anisotropic character of ZnS phase transformation and oxidation process is found.

© 2013 Elsevier B.V. All rights reserved.

## 1. Introduction

Today ZnS phosphors attract a great attention [1–7] because of their efficient emission in wide spectral region as well as their relative cheapness and simplicity of conventional methods of their synthesis. They are currently employed in many areas. In particular, these phosphors have been applied in electronic display devices, pigments in phosphorescent paints, electroluminescence devices and cathode ray tube equipment [8–11]. Powder ZnS-based electroluminescence devices with white emission can be used in liquid crystal display backlights such as cellular phones, personal digital assistants and palmtop computers. For white emission generation it is necessary to obtain the luminescence in blue or green spectral regions in addition to red emission. The emission of ZnS phosphors in blue–green spectral regions can be obtained by Cu doping, which results in appearance of green and/or blue broad bands centred at 505–530 nm and 440–465 nm, respectively [2 (and Ref. therein), 5, 12]. Because of this the luminescence properties of ZnS phosphors, including Cu doped

powder-like one, was intensively investigated in recent years [5–7,13–16]. It is known that ZnS emission characteristics depend on the sample fabrication and doping methods as well as on subsequent treatment.

One of the suitable methods to prepare phosphor materials based on zinc sulphide is a self-propagating high temperature synthesis (SHS) [17]. Technological capabilities of SHS are very broad, because it allows producing single-crystal and powders, including nanoscale materials, and doping them during synthesis. The SHS is an environmental friendly, low power consumption and low-cost method that can be applied for a large scale production of ZnS powders. These materials can be used as electro-, photo- and X-ray luminophore [18–21]. SHS method at last years attracts the attention because it allows preparation of ZnS powder with photoluminescence (PL) intensity comparable to that of commercial one [20]. At the same time, a number of issues for dispersed materials obtained by this method are not well addressed. Among them the next ones should be pointed out: localization of impurity, introduced during synthesis, and the influence of annealing on luminescence and structural characteristics of powders.

It is known that activator distribution is one of the most important factors determining the emission properties of phosphors. On the other hand, the heat treatment is the wide used procedure in

\* Corresponding author. Tel.: +380 66 1588840.

E-mail address: [an.kuchuk@gmail.com](mailto:an.kuchuk@gmail.com) (A. Kuchuk).

device fabrication processes. Specifically, the synthesized ZnS powder is heat treated for encapsulation (creation a ZnO layer), stress relaxation, doping, and a more homogeneous distribution of impurities inside the grains [22,23]. At the same time, the heat treatment can change the phase composition of phosphorus and the grain size [5,24–26], which also can affect the emission characteristics of the material. Therefore the investigation of the processes, which occurs at different annealing conditions, is important.

Usually the effect of temperature and duration of annealing, as well as cooling time of the ZnS materials, is studied [5,25,27]. At the same time it has been recently shown [28] that the variation of heating time to annealing temperature can also influence PL characteristics of powder-like ZnS. Specifically, this can control the intensity ratio of blue and green copper-related bands upon doping of ZnS with Cu from the surface (from CuCl).

In this paper similar effect was found also for the samples doped under synthesis. To elucidate its reason as well as the impurity localisation and phase composition of powder-like ZnS prepared by the SHS and doped by Cu in the growing process the luminescent and structural characteristics of the samples were studied before and after annealing. The formation of  $\text{Cu}_x\text{Zn}_{1-x}$  solid solution during synthesis is found. The latter affects significantly the luminescent properties of powder-like ZnS:Cu phosphors. The obtained results can be used for optimization of the doping technology and achievement the reproduction of the luminescent characteristics of the powders, obtained by SHS method.

## 2. Experimental details

ZnS:Cu powder was prepared by SHS method and doped during the growth process from the mixture with molar concentration of Zn–0.45, S–0.56, CuCl–0.006. The post growth thermal annealing of powders was carried out at 800 °C in quartz furnace. To restrict the access of atmospheric air we used a gas valve made of activated carbon. The annealing time was 120 min and heating time ( $t_h$ ) varied from 15 to 240 min.

Photoluminescence spectra were measured using an SDL-2 system at room temperature. PL was excited by the 337 nm line of  $\text{N}_2$  laser. X-ray diffraction (XRD) study was carried out using Philips X'Pert-MRD diffractometer with Cu  $K\alpha$ -radiation,  $\lambda=0.15418$  nm, in Bragg–Brentano geometry.

## 3. Results

### 3.1. PL characteristics

The PL spectra of initial and annealed samples are shown in Fig. 1a. The PL spectra of initial sample consist of broad band in blue–green spectral region with peak position at 510 nm and the shoulder at near 460 nm. The annealing results in the spectral shift of observed band and in the change of its full width at half maximum (FWHM), which depend on  $t_h$ . With  $t_h$  increase, the maximum position of PL band shifts firstly to the red and then to the blue spectral region, while its FWHM firstly decreases and then increases. These facts as well as the presence of the shortwave shoulder mean that the observed PL band is non-elementary. The deconvolution of PL spectra by the Gaussian approximation of initial and annealed at  $t_h=240$  min samples is shown in Fig. 1b by dotted lines. It is seen, that observed PL band consist of blue (B) and green (G) Cu-related bands with peak positions at 465 nm and 530 nm, respectively, as well as the self-activated (SA) band with peak position at 505 nm [29]. The dependences of these bands integral intensities on  $t_h$  are shown in Fig. 2. When  $t_h$  increases, the intensity of G-band at first increases, then, when  $t_h > 30$  min,

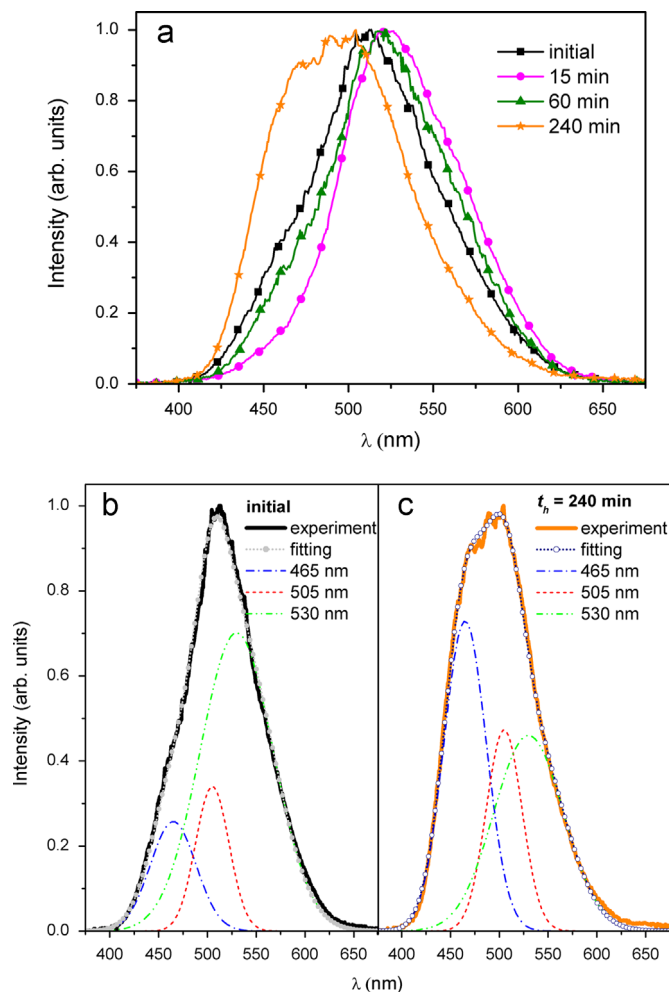


Fig. 1. Normalized PL spectra of the ZnS:Cu: (a) initial and annealed with different heating time at  $T=800$  °C (120 min); (b) and (c) deconvolution of PL bands for initial and treated at  $t_h=240$  min samples, respectively.

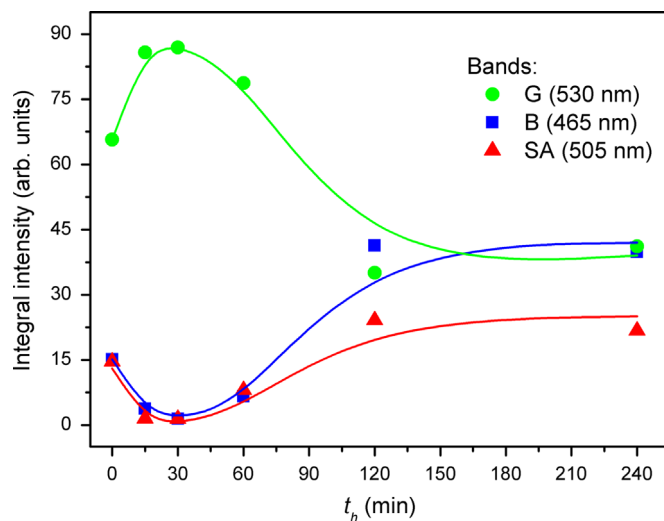


Fig. 2. The dependencies of integral intensities of Cu-related and self-activated bands on heating time. Point 0 at  $t_h$ -axis corresponds to initial sample.

decreases up to  $t_h=120$  min and after this does not change. At the same time the intensities of other two bands demonstrate the opposite dependence on  $t_h$  in the interval 15–120 min. From these data it can be concluded that the main reason of PL band

spectral shift is the change of contribution of Cu-related G- and B-bands to PL spectra. In fact, the red shift corresponds to the increase of G-band intensity while the intensity of B- and SA-bands decreases. At the same time blue shift corresponds to enhancement of B- and SA-bands. Because the peak position of observed PL-band at long  $t_h$  is at shorter wavelength than peak position of SA-band, blue shift is obviously caused by the increase of B-band intensity.

### 3.2. XRD patterns

XRD patterns of initial and annealed samples are shown in Fig. 3. The initial sample is a mixture of ZnS cubic (equilibrium) and ZnS hexagonal (non-equilibrium) phases. Besides, in this sample the peaks at  $2\theta \sim 36.3$ ;  $39$ ;  $43.2$  and  $54.3^\circ$  which can correspond to metallic Zn or to Zn-based solid solution ( $\text{Cu}_x\text{Zn}_{1-x}$  with  $x < 20\%$ ) with hexagonal Mg-like lattice [30] are observed. The coherent domain size ( $D$ ) of Zn or  $\text{Cu}_x\text{Zn}_{1-x}$  crystals, estimated from XRD patterns using the classical Scherrer formula, is about 30 nm. The presence of metallic-related phase results most likely from the non-equilibrium conditions of crystal growth.

The annealing gives rise to the changes of ZnS powder phase composition, which depend on  $t_h$ . In particular, the increase of  $t_h$  results in the decrease of ZnS hexagonal phase content, that is usually observed for ZnS phase mixture. Fig. 4a shows the hexagonal phase percentage versus  $t_h$  estimated using the method proposed in [31]. This dependence gives the evidence that cubic ZnS phase dominates both in initial and annealed samples. Its contribution in initial samples is about 87% and increases after annealing up to 95% at  $t_h = 240$  min.

Besides the decrease of hexagonal phase contribution, the annealing results in other transformation in XRD patterns. Specifically, after annealing reflections related to Zn or  $\text{Cu}_x\text{Zn}_{1-x}$  ( $x < 20\%$ ) hexagonal phases disappear and reflections from  $\text{Cu}_x\text{Zn}_{1-x}$  cubic phase with higher Cu content and from ZnO hexagonal phase arise.

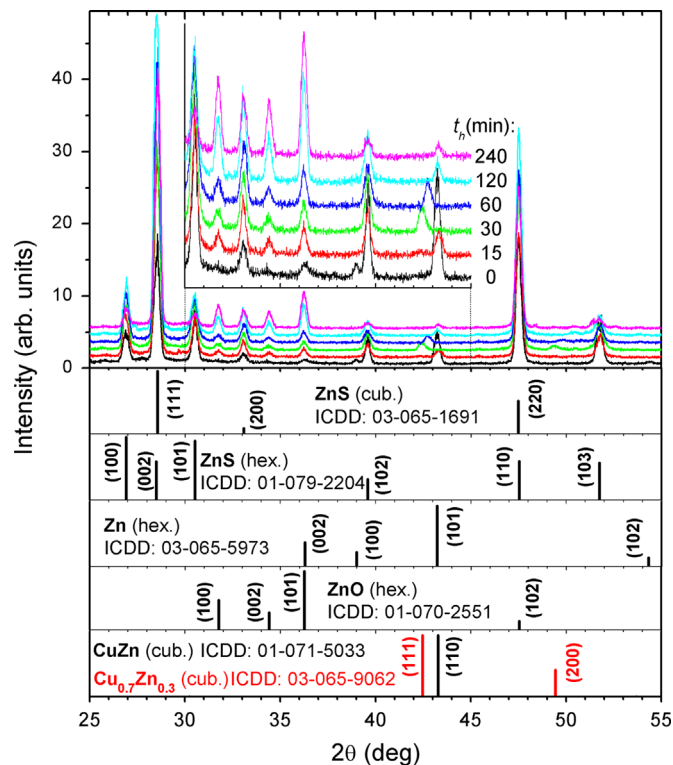


Fig. 3. XRD patterns of initial ZnS:Cu sample and the samples annealed with different heating time at  $T = 800^\circ\text{C}$  (120 min). At the bottom reference patterns for cubic ZnS,  $\text{Cu}_x\text{Zn}_{1-x}$  hexagonal ZnS, Zn and ZnO phases.

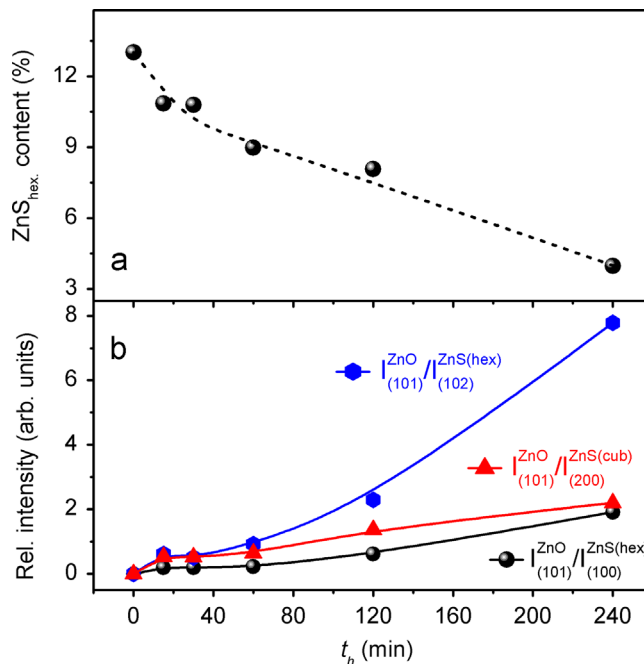


Fig. 4. The dependencies on heating time of (a) ZnS hexagonal phase content and (b) intensity ratios of 101 reflection from ZnO to 100 and 102 reflections from ZnS hexagonal phase and to 200 reflection from ZnS cubic phase.

In general, the latter can be caused by oxidation of ZnS as well as Zn or  $\text{Cu}_x\text{Zn}_{1-x}$  due to presence of oxygen in annealing atmosphere. Fig. 4b shows the dependencies of ratio of ZnO(1 0 1) reflection intensity to the intensities of ZnS(1 0 2) and ZnS(1 0 0) hexagonal phase reflections as well as to the intensity of ZnS(2 0 0) cubic phase reflection. It is seen, that the contribution of ZnO is insignificant at short heating time ( $t_h < 30$  min) and increases at higher  $t_h$ , that is most pronounced for ZnS(1 0 2) hexagonal phase reflection. The different slopes of  $t_h$  dependencies for different hexagonal phase reflections (Fig. 4b) mean that the process of hexagonal phase oxidation is anisotropic and testifies to the essential contribution of ZnS oxidation in ZnO formation.

As concerns the  $\text{Cu}_x\text{Zn}_{1-x}$  cubic phase with different Cu content is most likely formed from  $\text{Cu}_x\text{Zn}_{1-x}$  hexagonal phase with  $x < 20\%$ . This implies that reflections observed in initial sample originate rather from  $\text{Cu}_x\text{Zn}_{1-x}$  hexagonal phase than from pure metallic Zn. Let us consider the transformation of  $\text{Cu}_x\text{Zn}_{1-x}$  phase composition under annealing with different  $t_h$  in details. The annealing with  $t_h = 15$  min leads to the decrease of Zn content in solid solution and, as a result, to the formation of stoichiometric  $\text{Cu}_x\text{Zn}_{1-x}$  ( $x \approx 50\%$ ) phase with cubic lattice of CsCl type [30]. For this alloy the most intensive peak is for 110 reflection at  $2\theta \sim 43.2^\circ$ . The annealing with  $t_h = 30$  min causes the further Zn loss and formation of  $\text{Cu}_x\text{Zn}_{1-x}$  ( $x \approx 70\%$ ) phase with cubic lattice of NaCl type [30]. For this alloy 111 and 200 reflections at  $2\theta \sim 42.4$  and  $49.4^\circ$ , respectively, are the most intensive. The shift of these peaks to the larger angles after annealing at  $t_h = 30$ – $120$  min indicates that Cu content in  $\text{Cu}_x\text{Zn}_{1-x}$  solid solution decreases while the lattice remains of NaCl cubic type. The increase of  $t_h$  over 120 min does not lead to the further changes of  $\text{Cu}_x\text{Zn}_{1-x}$  phase composition. Thus, when  $t_h$  increases, the content of Cu in  $\text{Cu}_x\text{Zn}_{1-x}$  phase firstly increases and then decreases, that results in the non-monotone shift of  $\text{Cu}_x\text{Zn}_{1-x}$ -related peak position (Fig. 5). It should be noted that  $\text{Cu}_x\text{O}_{1-x}$  and  $\text{Cu}_x\text{S}_{1-x}$  phases were not observed both in the initial and the annealed samples.

The change of the phase composition in powder-like ZnS with the increase of  $t_h$  also results in the changes of  $D$  in cubic and hexagonal phases. As one can see from Fig. 6a, the  $D$  value, estimated

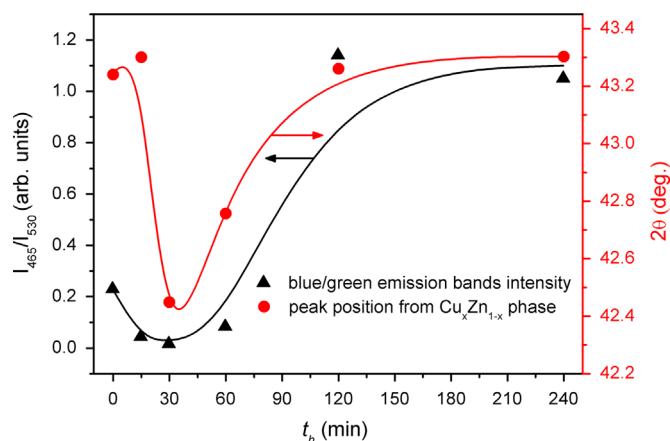


Fig. 5. The dependence of position of diffraction peak from  $\text{Cu}_x\text{Zn}_{1-x}$  phases and the ration of blue to green Cu-related band intensities on heating time.

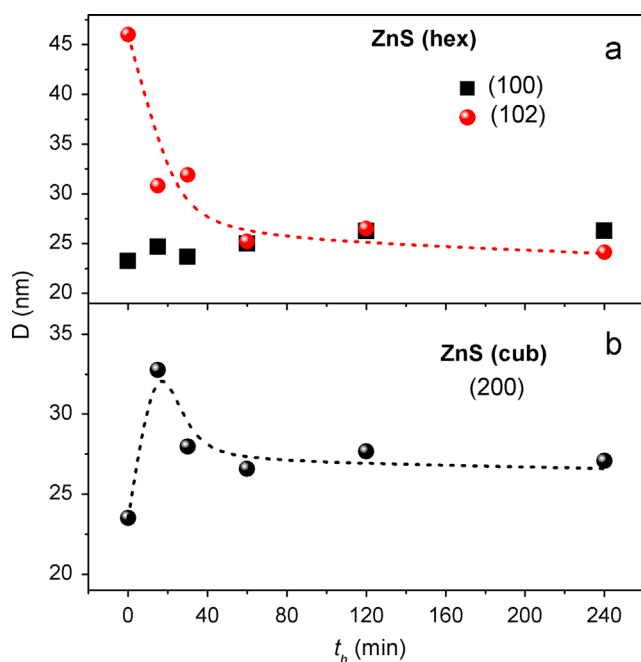


Fig. 6. The dependence of coherent domain size ( $D$ ) on heating time ( $t_h$ ): (a) ZnS with hexagonal structure; (b) ZnS with cubic structure.

by Scherrer formula, for ZnS with hexagonal structure evaluated from 102 reflection decreases with  $t_h$  increase, meanwhile this value determined from 100 reflection does not practically change. In ZnS crystals with cubic structure (see Fig. 6b) the  $D$  value at first increases and then decreases with  $t_h$  increase.

## 4. Discussion

### 4.1. Phase composition

The characteristic feature of obtained ZnS:Cu powder is the presence of  $\text{Cu}_x\text{Zn}_{1-x}$  alloy besides two ZnS phases. This demonstrates that, not all Cu atoms incorporate in ZnS microcrystals during synthesis in spite of the Cu concentration does not exceed the solution limit. In fact, as it will be shown below, the additional Cu atoms incorporate in ZnS microcrystals upon annealing, but the appearance of  $\text{Cu}_x\text{S}_{1-x}$  phase is not observed (see Section 3.2).

The annealing leads to the decrease of hexagonal and increase of cubic phase content, the oxidation owing to the oxygen presence in

the annealing ambience and the change of  $\text{Cu}_x\text{Zn}_{1-x}$  alloy composition. In general, the decrease of hexagonal phase content can be caused by transformation of the hexagonal phase into the cubic one as well as by more intensive oxidation of hexagonal phase in comparison with cubic one. The obtained results show that both these factors are responsible for the decrease of hexagonal phase content. This follows from the  $D(t_h)$  dependencies as well as from the intensity ratio of the ZnO(1 0 1) reflection to different ZnS reflections. In fact, more sharp dependence of the intensity ratio of ZnO(1 0 1) reflection to ZnS(1 0 2) hexagonal phase reflection on  $t_h$  in comparison with such a dependence for ZnS(2 0 0) cubic phase reflection (Fig. 4b) allows concluding that oxidation of the hexagonal phase is more intensive than the oxidation of the cubic one at least in one direction. Thus, this is one of the reasons why the hexagonal phase contribution decreases.

On the other hand, the phase transformation and oxidation will also result in the change of the  $D$  value. In general case the dependence of  $D$  versus  $t_h$  will be determined by the contribution of these two processes. Specifically, if the oxidation process is insignificant, the transformation of ZnS hexagonal phase to the cubic one will result in the increase of  $D$  value for cubic phase and its decrease for hexagonal one. Exactly this situation is observed at short  $t_h$  (Fig. 6). At the same time, the oxidation process will result in the decrease of  $D$  value both for cubic and hexagonal phases. So, superposition of both processes will lead to non-monotonic change of  $D$  for cubic phase and to the decrease of  $D$  value for hexagonal one, that was really observed for ZnS(2 0 0) cubic and ZnS(1 0 2) hexagonal phase reflections. The different  $D(t_h)$  dependencies evaluated from different reflections of hexagonal phase implies the anisotropy of both processes and it is in agreement with the slopes of curves in Fig. 4b.

It should be noted that the coherent domain size  $D$  determined by Scherrer formula for both ZnS phases (20–50 nm) was essentially smaller than microcrystals size (2–6  $\mu\text{m}$ ) obtained using the scanning electron microscopy. Thus, inside the microcrystals a considerable quantity of interphase boundaries is present. Therefore, it can be supposed that ZnS phase transformation and oxidation processes occur inside one microcrystal. The first phenomenon, as well as anisotropy of process, was observed in nanosized ZnS [31]. It should be noted, that the oxidation can hamper the ZnS phase transformation. This can explain why the  $D$  value increase in cubic phase is observed only at short  $t_h$ .

### 4.2. PL characteristics

The annealing results in considerable changes in PL characteristics of obtained ZnS powder. Based on the XRD and PL data, the model, that explains these changes can be proposed. Fig. 2 demonstrates that the dependence of G-band intensity on  $t_h$  in the interval 15–120 min has an opposite behavior to such dependencies for B- and SA-bands. This means that the variation of band intensities is due to redistribution of non-equilibrium carrier recombination flows between corresponding recombination centers (G-, B- and SA-centers). It is caused evidently by the changes in these centers' concentration. In particular, the increase of G-band intensity at short  $t_h$  can be due to the increase of G-centers concentration, that are  $\text{Cu}_{\text{Zn}}$ , or by the decrease of B- and SA-centers concentration. In these cases the number of non-equilibrium carriers, which can recombine through G-centers, will increase. Because the simultaneous concentration decrease of two emission centers of different nature is unlikely, we can conclude that the increase of G-band intensity is caused by the increase of G-center number. At the same time, this increase has to result in the decrease of both other band intensities, which is really experimentally observed. The increase of G-center concentration at

$t_h = 15\text{--}30$  min is obviously caused by diffusion of Cu atoms from  $\text{Cu}_x\text{Zn}_{1-x}$  phase into ZnS microcrystals.

To elucidate the reasons of other changes in PL characteristics let us compare them with the changes in XRD data. As it is shown in Fig. 5, the non-monotonic change of blue/green emission band intensity correlates with non-monotonic shift of XRD peak position from  $\text{Cu}_x\text{Zn}_{1-x}$  solid solution, i.e. with  $\text{Cu}_x\text{Zn}_{1-x}$  composition. The disappearance of reflections at  $2\theta \sim 36.3, 39$  and  $54.3^\circ$  as well as weakening of reflections at  $2\theta \sim 43.2$  at  $t_h \leq 30$  min testify to the decrease of Zn content in  $\text{Cu}_x\text{Zn}_{1-x}$  solid solution. Three possible reasons can be responsible for this phenomenon: evaporation and oxidation of Zn, if  $\text{Cu}_x\text{Zn}_{1-x}$  phase is located at the microcrystal surface, and Zn indiffusion. Because the formation of ZnO is insignificant at short  $t_h$ , the other two processes can be prevalent in this case. Since Zn diffusion coefficient in ZnS is high enough the diffusion process can be pronounced.

At longer  $t_h$  the decrease of Cu content in  $\text{Cu}_x\text{Zn}_{1-x}$  solid solution is dominant, which is accompanied by the decrease of  $\text{Cu}_x\text{Zn}_{1-x}$  related peak intensity. Because the evaporation of Zn from  $\text{Cu}_x\text{Zn}_{1-x}$  alloy under heating always dominates, and formation of Cu-oxides phases was not observed, it can be concluded that the main process, which leads to Cu content decrease, is Cu diffusion into ZnS microcrystals.

Thus, the incorporation of additional Cu atoms in ZnS microcrystals from  $\text{Cu}_x\text{Zn}_{1-x}$  phase takes place at all  $t_h$ . In this case the increase of, at least, one Cu-related PL band intensity due to formation of corresponding radiative centers is expected. At the short  $t_h$  this is G-band, but at  $t_h > 30$  min this is B-band. The formation of different recombination Cu-related centers at different  $t_h$  can be caused by the influence of Zn diffusion into ZnS microcrystals. In fact, because the decrease of Zn content in  $\text{Cu}_x\text{Zn}_{1-x}$  phase dominates at  $t_h < 30$  min, we can conclude that in this case Cu diffusion into ZnS is accompanied by Zn diffusion. At the same time, the decrease of Cu content in alloy prevails at  $t_h > 30$  min, which implies Cu diffusion to be dominant.

These facts allow explaining the dependence of PL characteristics on  $t_h$  by the next way. It is well known that the relation of blue/green emission bands intensities upon doping depends on the relation of Cu/coactivator concentration  $N_{\text{Cu}}/N_c$  [12]. If  $N_{\text{Cu}}/N_c \leq 1$ , green emission is observed. At the same time, blue emission appears when  $N_{\text{Cu}}/N_c > 1$ . In this case formation of  $\text{Cu}_{\text{Zn}}\text{--Cu}_i$  complexes, that are centers responsible for blue emission [32], can take place due, apparently, to Cu self compensation, i.e. compensation of  $\text{Cu}_{\text{Zn}}$  acceptors by  $\text{Cu}_i$  donors. Since  $\text{Zn}_i$  can play role of coactivator, the relation  $N_{\text{Cu}}/N_c \leq 1$  is obviously realized at short  $t_h$ . This will result in the enhancement of green emission and the shift of PL band to the long wavelength side. At long  $t_h$  Cu diffusion from alloy dominates. Thus, in this case the relation  $N_{\text{Cu}}/N_c > 1$  takes place, which leads to enhancement of blue emission band and to the shift of PL band position to the short wavelength side. The increase of  $\text{Cu}_i$  concentration in ZnS due to Cu diffusion from  $\text{Zn}_x\text{Cu}_{1-x}$  phase can also result in the formation of complexes  $\text{Cu}_{\text{Zn}}\text{--Cu}_i$  with G-centers which were present in ZnS. This has to lead to the decrease of G-centers concentration. Thus, the decrease of G-band intensity at  $t_h > 30$  min is apparently caused not only by the increase of B-center number but also by the decrease of G-center concentration. The latter can be the main reason of the increase of SA-band intensity, while two reasons (decrease of G-centers and increase of B-center concentration) determine the enhancement of B-band. This is confirmed by the more pronounced increase of B-band intensity in comparison of SA-band one.

Thus, the presence of  $\text{Cu}_x\text{Zn}_{1-x}$  phase, which was formed during synthesis of ZnS:Cu powder, is responsible for dependence of its PL characteristics on heating time. The formation of this phase is caused obviously by the fast reaction between free Zn and Cu, so the formation of  $\text{Cu}_x\text{Zn}_{1-x}$  phase occurs faster than

complete incorporation of Cu into ZnS microcrystals. It should be noted that additional annealing of ZnS:Cu powder, which contains  $\text{Cu}_x\text{Zn}_{1-x}$  phase, allows controlling the relation between intensities of green and blue Cu-related bands. On the other hand, its presence should be taken into account when Cu doped powders are submitted to additional thermal treatment.

## 5. Conclusions

The luminescent and structural characteristics of the powder-like ZnS:Cu prepared by SHS from the mixture of Zn, S and CuCl and influence of annealing at  $800^\circ\text{C}$  on them were investigated. In XRD patterns  $\text{Cu}_x\text{Zn}_{1-x}$  phase was revealed in addition to ZnS cubic and hexagonal phases. PL spectra demonstrate a broad band, which is the superposition of blue and green Cu-related bands as well as self-activated one.

It was found that annealing results in next changes of ZnS powder phase composition which depend on heating time to annealing temperature: the decrease of ZnS hexagonal phase content and the increase of cubic one, the appearance and increase of ZnO phase content as well as non-monotonic change of  $\text{Cu}_x\text{Zn}_{1-x}$  alloy composition. It is shown that oxidation process is anisotropic and more pronounced for hexagonal ZnS phase. The change of XRD coherent domain size in both ZnS phases testifies to the anisotropic character of ZnS phase transformation. In PL spectra the non-monotonic shift of PL peak position versus heating time is found. It is shown, that this shift is caused by the changes in concentrations of recombination centers responsible for green and blue Cu-related bands and correlates with the change of  $\text{Cu}_x\text{Zn}_{1-x}$  phase composition. The model that explains the changes of PL characteristics by diffusion of Zn and Cu into ZnS microcrystals from  $\text{Cu}_x\text{Zn}_{1-x}$  alloy is proposed.

## References

- [1] A.A. Khosravi, M. Kundu, L. Jatwa, S.K. Deshpande, U.A. Bhagwat, M. Sastry, S. K. Kulkarni, *Appl. Phys. Lett.* 67 (18) (1995) 2702.
- [2] W.Q. Peng, Y.W. Cong, S.C. Oiu, Z.Y. Wang, *Opt. Mater.* 29 (2–3) (2006) 313.
- [3] S. Hana, I. Singh, D. Singh, Y. Lee, Y. Sharma, C. Han, *J. Lumin.* 115 (1) (2005) 97.
- [4] M. Warkentin, F. Bridges, S.A. Carter, M. Anderson, *Phys. Rev. B: Condens. Matter* 75 (2007) 075301.
- [5] W. Wang, F. Huang, Y. Xia, A. Wang, J. Yang, *M.R.S. Bull.* 43 (7) (2008) 1892.
- [6] Y.-T. Nien, I.-G. Chen, *Appl. Phys. Lett.* 89 (26) (2006) 261906.
- [7] Y.-T. Nien, I.-G. Chen, C.h.-S.h. Hwang, S.h.-G. Chu, *J. Phys. Chem. Solids* 69 (2–3) (2008) 366.
- [8] A.R. Mirhabibi, M. Rabiee, R. Aghababazadeh, F. Moztafzadeh, S. Hesaraki, *Pigm. Resin Technol.* 32 (2003) 358.
- [9] Ph.D. Rack, P.H. Holloway, *Mater. Sci. Eng. R. Rep* R21 (1998) 171.
- [10] J. Banga, B. Abrams, *J. Appl. Phys.* 95 (2004) 7873.
- [11] J.H. Park, S.H. Lee, J.S. Kim, A.K. Kwon, H.L. Park, S.D. Han, *J. Lumin.* 126 (2007) 566.
- [12] M. Aven, J.S. Prener, *Physics and Chemistry of II–VI Compounds*, N.Y., North-Holland, Wiley-VCH, Amsterdam (1967) 464.
- [13] Y.-T. Nien, I.-G. Chen, C.-S. Hwang, S.-J. Chu, *J. Electroceram.* 17 (2006) 299.
- [14] M.M. Sychoy, K.A. Ogurtsov, T.V. Lebedev, Y.u.V. Kulvelis, G.y. Tork, A.E. Sokolov, V.A. Trunov, V.V. Bakhmetyev, A.A. Kotomin, S.A. Dushenok, A.S. Kozlov, *Semiconductors* 46 (5) (2012) 696.
- [15] S. Ummartyotin, N. Bunnak, J. Juntaro, M. Sain, H. Manuspiya, *Solid State Sci.* 14 (2012) 299.
- [16] W. Wang, F. Huang, Y. Xia, A. Wang, *J. Lumin.* 128 (2008) 610.
- [17] S.V. Kozytckyy, V.P. Pysarskyy, D.D. Polishchuk, *Phys. Chem. Solid State* 4 (2003) 749.
- [18] C.W. Won, H.H. Nersisyan, H.I. Won, D.Y. Jeon, J.Y. Han, *J. Lumin.* 130 (2010) 1026.
- [19] S.V. Kozytckyy, *J. Appl. Spectrosc.* 63 (1) (1996) 101.
- [20] H. Tanaka, E. Miyazaki, O. Odawara, J. Self, *Propag. High Temp. Synth* 13 (3) (2004) 227.
- [21] S.V. Kozitskii, A.P. Chebanenko, *J. Appl. Spectrosc.* 60 (5–6) (1994).
- [22] H.R. Luxenberg, Rudolph L. Kuehn (Eds.), *Display Systems Engineering*, McGraw-Hill Book Company, N.Y., San-Francisco, Toronto, London, Sydney, 1968.
- [23] A.N. Georgobiani, *Soviet Physics Uspekhi* 17 (4) (1974) 424.
- [24] Po-Chang Lin, Chi Chung Hua, Tai-Chou Lee, *J. Solid State Chem.* 194 (2012) 282.
- [25] T. Kryshtab, V.S. Khomchenko, J.A. Andraca-Adame, V.B. Khachatryan, M.O. Mazin, V.E. Rodionov, M.F. Mukhliu, *J. Cryst. Growth* 275 (1) (2005) 1163.
- [26] Wei Zhang, Xianghua Zeng, Hongfei Liu, Junfeng Lu, *J. Lumin.* 134 (2013) 498.

- [27] N.I. Khinev, M.M. Grebenyuk, V.G. Kanibolotskii, *Izvestiya VisshikhUchebnukh Zavedenii, Fizika*, № 6, 733, 1971.
- [28] Yu.Yu. Bacherikov, I.S. Golovina, N.V. Kitsyuk, *Phys. Solid State* 48 (10) (2006) 1872.
- [29] V.F. Tunitskaya, T.F. Filina, E.I. Panasyuk, Z.P. Ilyuhina., *Ser. Phys.* 35 (1987) 1437.
- [30] S.M. Barabash, Yu.N. Koval. *Structure and Properties of Metals and Alloys*, Naukova Dumka, Kiev, 1986.
- [31] F. Huang, J.F. Banfield, *ACS* 127 (2005) 4523.
- [32] N. Riehl, R. Sizmann, in: H.P. Kallman, G.M. Spruch (Eds.), *Luminescence of Organic and Inorganic Materials*, Willey, 1962, p. 344.